NUKLEONIKA 2017;62(2):135–140
doi: 10.1515/nuka-2017-0019

ORIGINAL PAPER

Hyperfine interactions and some thermomagnetic properties of amorphous FeZr(Cr)NbBCu alloys

Agnieszka Łukiewska, Jacek Olszewski

Abstract. In this research, we studied the magnetic phase transition by Mössbauer spectroscopy and using vibrating sample magnetometer for amorphous $Fe_{86-x}Zr_7Cr_xNb_2Cu_1B_4$ (x = 0 or 6) alloys in the as-quenched state and after accumulative annealing in the temperature range 600–750 K. The Mössbauer investigations were carried out at room and nitrogen temperatures. The Mössbauer spectra of the investigated alloys at room temperature are characteristic of amorphous paramagnets and have a form of asymmetric doublets. However, at nitrogen temperature, the alloys behave like ferromagnetic amorphous materials. The two components are distinguished in the spectrum recorded at both room and nitrogen temperatures. The low field component in the distribution of hyperfine field induction shifts towards higher field with the annealing temperature. It is assumed that during annealing at higher temperature, due to diffusion processes, the grains of α-Fe are created in the area corresponding to this component. Both investigated alloys show the invar effect and the decrease of hyperfine field induction after annealing at 600 K for 10 min is observed. It is accompanied by the lowering of Curie temperature.

Keywords: amorphous Fe-based alloys • invar effect • Mössbauer spectroscopy

Introduction

Fe-based amorphous alloys are attractive since they exhibit excellent soft magnetic properties combined with high saturation magnetization. Fe-Zr- and Fe-Cr-based amorphous alloys are one of the groups of these materials and show complex magnetic structure and numerous anomalies [1, 2], i.e. spin-glass, re-entrant spin-glass and invar effect. These anomalies are observed at low temperatures. Due to the lack of the long-range order of atoms in amorphous materials, the exchange interaction between magnetic moment fluctuates which involves inhomogeneity of the local magnetization – spin frustration [3]. It is commonly known that the amorphous alloys are thermodynamically instable and their structure is changing during annealing even at relatively low temperature. Because of close correlation between the structure and properties of the amorphous alloys, their magnetic properties can be modified by the proper annealing [4]. Magnetic ordering of amorphous alloys is strongly affected by their chemical composition and temperature [5].

An excellent method for studying the microstructure, magnetic order and magnetization inhomogeneity of amorphous alloys is the Mössbauer spectroscopy because it permits one to elucidate

A. Łukiewska✉, J. Olszewski
Institute of Physics,
Czestochowa University of Technology,
19 Armii Krajowej Str., 42-200 Częstochowa, Poland,
Tel./Fax: +48 34 325 0795,
E-mail: aluk@wip.pcz.pl

Received: 21 June 2016
Accepted: 29 September 2016

the nature of both electric and magnetic hyperfine interactions of different resonating iron nuclei and to probe their immediate surroundings [6].

In amorphous alloys, both quadrupolar and magnetic Mössbauer spectra show the line broadening due to structural disorder and can be interpreted in terms of local disorder. In the magnetically ordered alloys containing Fe, the distribution of hyperfine field can be correlated with the distribution of Fe coordination.

The temperature of magnetic phase transition of amorphous alloys can be determined from thermomagnetic curves.

In this paper the results of structure and magnetic phase transition studies by Mössbauer spectroscopy and vibrating sample magnetometer (VSM) for amorphous $Fe_{86-x}Zr_7Cr_xNb_2B_4Cu_1$ ($x = 0$ or 6) alloys in the form of ribbons 3 mm wide and 20 μm thick prepared by a rapid solidification are presented.

Experimental procedure

Ingots of alloys with nominal compositions $Fe_{86-x}Zr_7Cr_xNb_2Cu_1B_4$ ($x = 0$ or 6) were prepared by melting of an appropriate amount of high purity elements in an arc melting furnace under the protective argon atmosphere. Obtained in this way, the samples were re-melted several times to achieve good homogeneity. Rapidly solidified ribbons were produced in the controlled argon atmosphere.

The microstructure of the as-quenched and annealed ribbons was studied by X-ray diffractometry and Mössbauer spectroscopy. A Bruker-AXS, type D8 Advanced X-ray diffractometer with Cu anode and conventional Mössbauer spectrometer with a $^{57}Co(Rh)$ radioactive source were used. The spectrometer was calibrated at room temperature with 20 μm thick α-Fe polycrystalline foil. The transmission spectra were recorded at room temperature (298 K) and nitrogen temperature (77 K). Mössbauer spectra were analysed by a Normos package according to the procedure developed in [7].

The temperatures of the magnetic phase transition (Curie temperature T_C) were obtained by the derivation of thermomagnetic curves recorded by means of a vibration sample magnetometer (VSM) VersaLab (Quantum Design) system in the temperature range from 50 K up to 400 K at the magnetizing field induction of 5 mT.

All studies were performed for pieces cut out from the ribbons in the as-quenched state and after accumulative annealing for 10 min at 600 K than at 700 K and 750 K in vacuum of 1.33×10^{-3} Pa.

Results and discussion

In Fig. 1 X-ray diffraction patterns for the samples of $Fe_{86}Zr_7Nb_2Cu_1B_4$ and $Fe_{80}Zr_7Cr_6Nb_2Cu_1B_4$ after the accumulative annealing for 10 min at 600 K and then 700 K are shown. Only broad halo without any evidence of sharp peaks corresponding to the crystalline phase is observed.

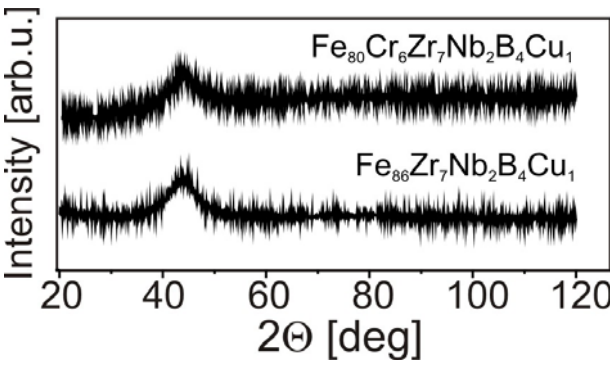

Fig. 1. X-ray diffraction patterns for the investigated alloys after annealing for 10 min at 700 K.

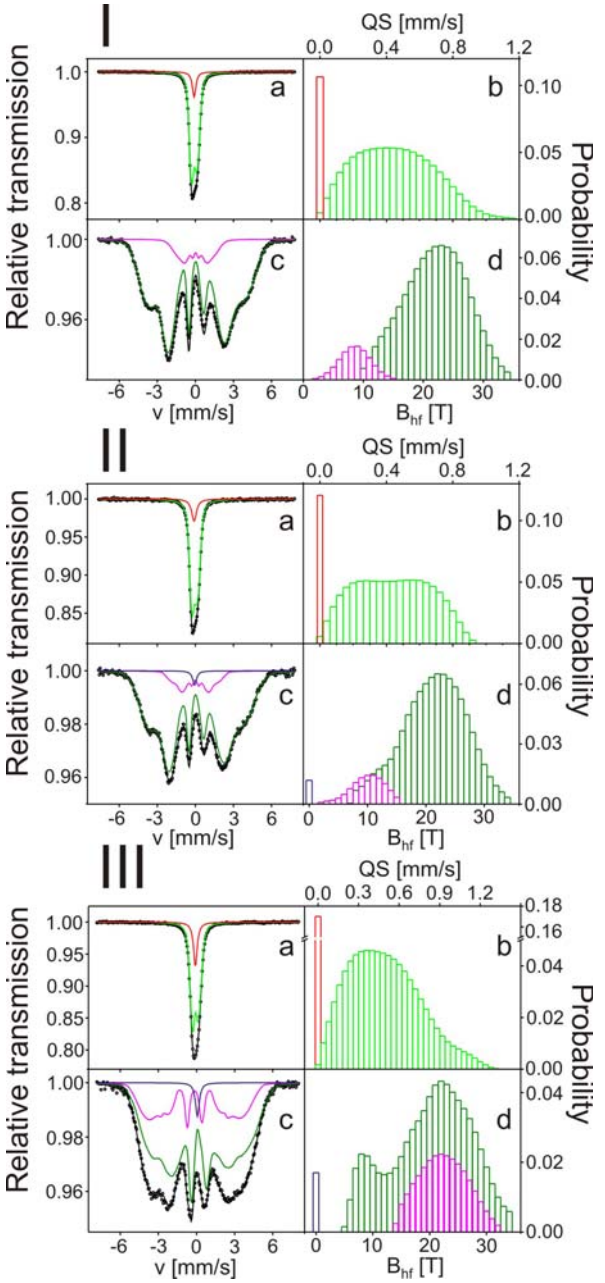

Fig. 2. Transmission Mössbauer spectra (a, c) and corresponding quadrupole splitting (b) and hyperfine field induction distributions (d) for $Fe_{86}Zr_7Nb_2Cu_1B_4$ alloy in the as-quenched state (asq) (I) and after heat treatment for 10 min at 600 K (II) and then at 700 K (III).

Transmission Mössbauer spectra measured at 298 K and 77 K for the as-quenched and annealed samples of $Fe_{86}Zr_7Nb_2Cu_1B_4$ alloy are presented in Fig. 2. The results obtained from Mössbauer spectra analysis are collected in Table 1. The Mössbauer spectrum of as-received sample recorded at room temperature is characteristic of amorphous paramagnetic alloys and has a form of the asymmetric doublet (Fig. 2.I-a). This spectrum can be decomposed into a distribution of symmetric doublets with linear correlation between isomer shift (IS) and quadrupole splitting (QS) [8, 9], and the single line (Fig. 2.I-b) with isomer shift equal to –0.10(1) mm/s (Table 1). This value of IS is close to that of fcc iron [10]. The Mössbauer spectrum of this sample recorded at 77 K is characteristic of amorphous ferromagnets and has a form of asymmetric sextets with broad and overlapped lines (Fig. 2.I-c). The spectrum can be presented as a sum of two distributions of symmetric sextets with linear correlation between IS and magnetic hyperfine field induction B_{hf} [8, 9]. It is worth noticing that the main component in the hyperfine field induction distribution (Fig. 2.I-d) has bimodal character with low and high field overlapped components, characteristic of ferromagnetic amorphous alloys [4].

The Mössbauer spectra and corresponding distributions of hyperfine parameters obtained for the sample of $Fe_{86}Zr_7Nb_2Cu_1B_4$ annealed at 600 K and then 700 K are depicted in Fig. 2.II and Fig. 2.III. From the analysis of these spectra performed in the same manner as for as-quenched sample, we have found that IS of the single line does not change after the annealing at 600 K and slightly increases after heat treatment at 700 K (Table 1). However, its relative intensity increases with annealing temperature (Table 1). The average QS of the quadrupole distribution at first decreases and then increases with annealing temperature. The similar relation is observed for average magnetic hyperfine field induction (B_{hf}) for $Fe_{86}Zr_7Nb_2Cu_1B_4$ samples measured at 77 K. The decrease of B_{hf} after annealing of sample at 600 K for 10 min is characteristic of materials exhibiting invar effect [11]. It is worth noticing that the average magnetic field induction ($<B_{hf}>_1$) of the main component decreases with annealing temperature. This is accompanied by a decrease of its intensity. Simultaneously, the separation of components in the main distribution of hyperfine field induction is observed (Fig. 2.II-d and Fig. 2.III-d). The average value of magnetic field induction ($<B_{hf}>_2$) and the relative intensity of the minor component increase with the annealing temperature (Table 1).

The Mössbauer spectrum of the sample after substitution 6% at Fe by Cr atoms only slightly changes at both room and nitrogen temperatures

Table 1. The average value of the quadrupole splitting distribution (QS) and its standard deviation (ΔQS), parameters of the linear dependence between QS and IS (IS_0 and a), average value of IS ($<IS>$), relative intensity of the QS distribution (I), isomer shift of the single line (IS_L) and its relative intensity (I_L), the relative intensity of the second and fifths line in sextet ($A_{2,5}$), average hyperfine field $<B_{hf}>$, average hyperfine field of components $<B_{hf}>_i$ their standard deviations $\Delta<B_{hf}>_i$, parameters of linear dependence between $(B_{hf})_i$ and IS_i (IS_{0i} and b_i), average value of IS_i ($<IS>_i$) and their relative intensities (I_i) (i = 1 and 2 for the main and minor components, respectively) of $Fe_{86}Zr_7Nb_2B_4Cu_1$ alloy in the as-quenched state (asq) and after accumulative heat treatment. Uncertainties for the last significant figure are given in brackets

Mössbauer spectra parameters	Sample treatments/measuring temperature					
	Asq/ Room temperature	Asq/ Nitrogen temperature	600 K/ Room temperature	600 K/ Nitrogen temperature	700 K/ Room temperature	700 K/ Nitrogen temperature
QS [mm/s]	0.4530(7)		0.438(2)		0.508(2)	
ΔQS [mm/s]	0.233(2)		0.221(3)		0.281(3)	
IS_0 [mm/s]	–0.1082(4)		–0.080(2)		–0.099(1)	
a	0.00249(3)		0.0025(2)		0.0021(1)	
$<IS>$ [mm/s]	0.06(4)		–0.05(1)		–0.07(2)	
I	0.90(2)		0.88(2)		0.83(2)	
IS_L [mm/s]	–0.10(1)		–0.10(1)	–0.061(3)	–0.089(2)	0.07(1)
I_L	0.10(2)		0.12(2)	0.02(2)	0.17(2)	0.02(2)
$A_{2,5}$		2.56(3)		2.67(5)		1.48(4)
$<B_{hf}>$ [T]		20.58(8)		20.19(4)		20.89(3)
$<B_{hf}>_1$ [T]		21.98(9)		21.40(3)		20.27(7)
$\Delta<B_{hf}>_1$ [T]		5.1(1)		5.4(3)		6.98(5)
$(IS_0)_1$ [mm/s]		–0.044(4)		–0.061(8)		0.03(1)
b_1 [mm·s^{-1}·T^{-1}]		0.008(3)		0.008(6)		0.008(1)
$<IS>_1$ [mm/s]		0.02(1)		0.05(4)		0.16(6)
I_1		0.90(2)		0.88(2)		0.75(2)
$<B_{hf}>_2$ [T]		8.6(4)		9.9(4)		22.7(1)
$\Delta<B_{hf}>_2$ [T]		2.5(5)		2.8(2)		3.91(6)
$(IS_0)_2$ [mm/s]		0.23(1)		0.001(1)		–0.17(2)
b_2 [mm·s^{-1}·T^{-1}]		0.00(2)		–0.001(1)		0.004(2)
$<IS>_2$ [mm/s]		–0.08(1)		–0.08(3)		–0.15(2)
I_2		0.10(2)		0.10(2)		0.23(2)

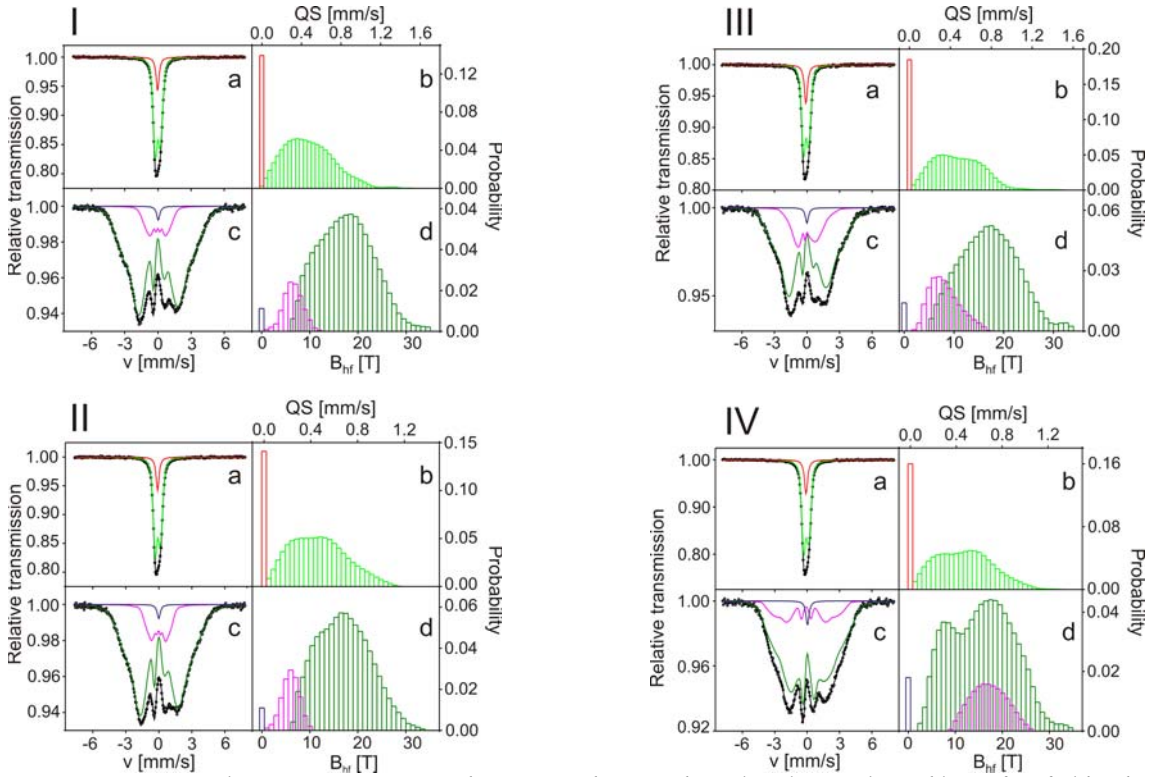

Fig. 3. Transmission Mössbauer spectra (a, c) and corresponding quadrupole splitting (b) and hyperfine field induction distributions (d) for $Fe_{80}Cr_6Zr_7Nb_2Cu_1B_4$ alloy in the as-quenched state (asq) (I) and after heat treatment for 10 min at 600 K (II), and then at 700 K (III) and 750 K (IV).

Table 2. The average value of the quadrupole splitting distribution (QS) and its standard deviation (ΔQS), parameters of the linear dependence between QS and IS (IS_0 and a), average value of IS ($<IS>$), relative intensity of the QS distribution (I), isomer shift of the single line (IS_L) and its relative intensity (I_L), the relative intensity of the second and fifths line in sextet ($A_{2,5}$), average hyperfine field $<B_{hf}>$, average hyperfine field of components $<B_{hf}>_i$ their standard deviations $\Delta<B_{hf}>_i$, parameters of linear dependence between $(B_{hf})_i$ and IS_i (IS_{0i} and b_i), average value of IS_i ($<IS>_i$) and their relative intensities (I_i) (i = 1 and 2 for the high and low field components, respectively) of $Fe_{80}Cr_6Zr_7Nb_2B_4Cu_1$ alloy in the as-quenched state (asq) and after accumulative heat treatment. Uncertainties for the last significant figure are given in brackets

Mössbauer spectra parameters	Sample treatments/measuring temperature					
	Asq/ Room temperature	Asq/ Nitrogen temperature	700 K/ Room temperature	700 K/ Nitrogen temperature	750 K/ Room temperature	750 K/ Nitrogen temperature
QS [mm/s]	0.482(2)		0.482(2)		0.482(2)	
ΔQS [mm/s]	0.256(3)		0.246(5)		0.250(3)	
IS_0 [mm/s]	–0.038(1)		–0.112(2)		–0.113(1)	
a	0.0023(9)		0.0025(2)		0.0026(1)	
$<IS>$ [mm/s]	–0.01(1)		–0.08(2)		–0.08(2)	
I	0.86(2)		0.82(2)		0.84(2)	
IS_L [mm/s]	–0.027(2)	0.03(1)	–0.101(2)	0.01(2)	–0.099(2)	0.04(2)
I_L	0.14(2)	0.01(2)	0.18(2)	0.02(2)	0.16(2)	0.02(2)
$A_{2,5}$		2.8(1)		3.0(1)		1.92(6)
$<B_{hf}>$ [T]		16.22(4)		15.37(5)		15.95(4)
$<B_{hf}>_1$ [T]		17.6(2)		17.2(2)		15.80(1)
$\Delta<B_{hf}>_1$ [T]		5.6(1)		5.6(1)		6.56(6)
$(IS_0)_1$ [mm/s]		–0.028(4)		–0.06(1)		–0.036(9)
b_1 [mm·s^{-1}·T^{-1}]		0.0066(4)		0.009(1)		0.0086(6)
$<IS>_1$ [mm/s]		0.04(3)		0.05(4)		0.07(5)
I_1		0.87(2)		0.78(2		0.82(2)
$<B_{hf}>_2$ [T]		6.4(4)		8.20(3)		17.0(3)
$\Delta<B_{hf}>_2$ [T]		2.1(3)		3.10(2)		3.50(3)
$(IS_0)_2$ [mm/s]		–0.02(2)		–0.14(3)		–0.096(4)
b_2 [mm·s^{-1}·T^{-1}]		0.001(4)		0.022(4)		0.04(1)
$<IS>_2$ [mm/s]		–0.08(2)		0.01(4)		–0.089(3)
I_2		0.12(2)		0.20(2)		0.16(2)

(Fig. 3). The appropriate fitting parameters obtained from the analysis of Mössbauer spectra for $Fe_{80}Zr_7Cr_6Nb_2Cu_1B_4$ alloy are listed in Table 2. It is seen that the addition of Cr atoms enhances average QS which is equal to 0.482 mm/s for the sample in the as-quenched state and does not change after annealing of the sample. Simultaneously, the decrease of average hyperfine field induction takes place as compared to $Fe_{86}Zr_7Nb_2Cu_1B_4$ alloy. The change of both average field induction $<B_{hf}>$ and average field inductions of components $<B_{hf}>_i$ have the same character as for $Fe_{86}Zr_7Nb_2Cu_1B_4$ alloy and invar effect is also observed.

Moreover, the isomer shift (IS) of the single line for as-quenched $Fe_{80}Cr_6Zr_7Nb_2Cu_1B_4$ sample is larger than for $Fe_{86}Zr_7Nb_2Cu_1B_4$ alloy. It may be caused by the change of Fe local symmetry from fcc-like to bcc-like symmetry with Cr atoms in the nearest neighbourhood [12]. After the annealing at 700 K, the isomer shift decreases up to –0.101(2) mm/s and remains constant after annealing at 750 K. It could be caused by the decrease of distances between Fe and Cr atoms or/and the increase of Cr concentration.

It is worth pointing out that the low field component in the hyperfine field induction distribution shifts towards higher fields. Furthermore, it can be assumed that after annealing at a higher temperature, the crystalline grains are created in the area corresponding to this component.

In order to determine the temperature of the magnetic phase transition (the Curie temperature T_C), the specific magnetization (σ) at the magnetizing field induction of 5 mT vs. temperature for the as-received alloys and after annealing was measured. To find the Curie point, the derivative $d\sigma/dT$ was numerically calculated (Fig. 4).

It can be seen that an addition of 6 at.% Cr to $Fe_{86}Zr_7Nb_2Cu_1B_4$ alloy causes lowering of T_C by 15 K. The Curie temperature distinctly decreases after annealing the samples at 600 K in comparison with the as-quenched state, and then, increases with annealing temperature (Fig. 4). This behaviour coincides with the change of average hyperfine field induction (Tables 1 and 2).

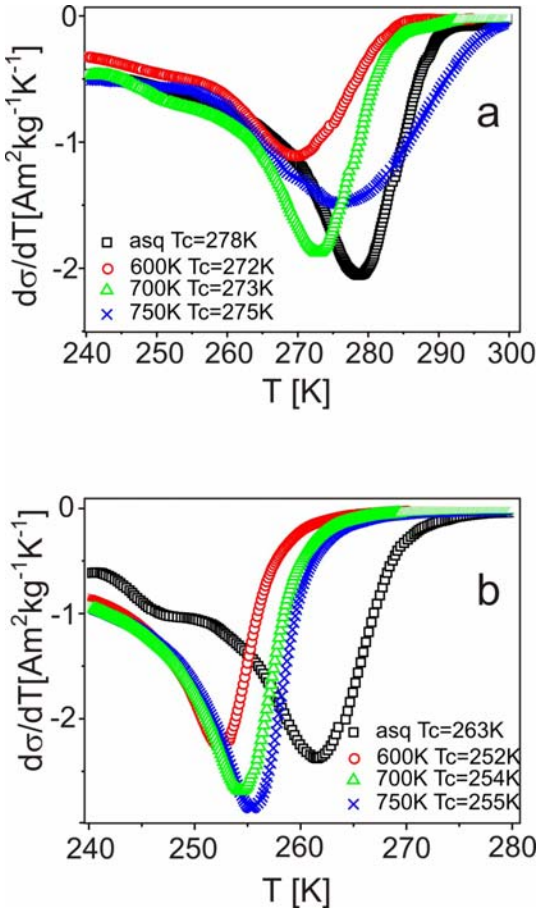

Fig. 4. Derivative of specific magnetization ($d\sigma/dT$) versus temperature for $Fe_{86}Zr_7Nb_2Cu_1B_4$ (a) and $Fe_{80}Cr_6Zr_7Nb_2Cu_1B_4$ (b) alloys in the as-quenched state (asq) and after annealing at 600 K, and then at 700 K and 750 K for 10 min, measured in the magnetizing field induction B = 5 mT.

Conclusions

- The investigated alloys at room temperature, in both as-quenched state and after accumulative annealing, are paramagnetic amorphous materials.
- The structure of alloys is complex and at least two components which are characterized by different QS_i at room temperature and $<B_{hf}>_i$ at nitrogen temperature can be distinguished.
- The average hyperfine field induction $<B_{hf}>_2$ of minor component increases with annealing temperature.
- It can be assumed that after the heat treatment above 760 K, the α-Fe grains will be created in the area corresponding to the minor component.
- Investigated alloys exhibit the invar effect and the decrease of the average hyperfine field induction after annealing at 600 K was observed.

References

1. Lorenz, R., & Hafner, J. (1995). Non-collinear magnetic structures in amorphous iron and iron-based alloys. *J. Magn. Magn. Mater.*, *139*, 209–227. DOI: 10.1016/0304-8853(95)90049-7.
2. Rzącki, J., Świerczek, J., Hasiak, M., Olszewski, J., Zbroszczyk, J., & Ciurzyńska, W. (2015). Hyperfine interaction and some thermomagnetic properties of amorphous and partially crystallized $Fe_{70-x}M_xMo_5Cr_4Nb_6B_{15}$ (M=Co or Ni, x=0 or 10). *Nukleonika*, *60*(1), 121–126. DOI: 10.1515/nuka-2015-0025.
3. Ren, H., & Ryan, D. H. (1995). Exchange frustration and transverse spin freezing in iron-rich metallic glasses. *Phys. Rev. B*, *51*, 15885–15897.
4. McHenry, M. E., Willard, M. A., & Laughlin, D. E. (1999). Amorphous and nanocrystalline materials for applications as soft magnets. *Prog. Mat. Sci.*, *44*, 291–433. DOI: 10.1016/S0079-6425(99)00002-X.
5. Herzer, G. (2013). Modern soft magnets: Amorphous and nanocrystalline materials. *Acta Mater.*, *61*, 718–734. DOI: 10.1016/j.actamat.2012.10.040.
6. Greneche, J. M. (1997). Nanocrystalline iron-based alloys investigated by Mössbauer spec-

trometry. *Hyperfine Interact.*, *110*, 81–91. DOI: 10.1023/A:1012671315478.
7. Miglierini, M., & Greneche, J. M. (1997). Mössbauer spectrometry of Fe(Cu)MB-type nanocrystalline alloys: I. The fitting model for the Mössbauer spectra. *J. Phys.-Condens. Matter*, *9*, 2303–2319. DOI: 10.1088/0953-8984/9/10/017.
8. Hesse, J., & Rübartsch, A. (1974). Model independent evaluation of overlapped Mössbauer spectra. *J. Phys. E.-Sci. Inst.*, *7*, 526–532.
9. Brand, R. A. (1987). Improving the validity of hyperfine field distributions from magnetic alloys. *Nucl. Instrum. Methods Phys. Res. Sect. B-Beam Interact. Mater. Atoms*, *28*, 398–416.
10. Kopcewicz, M., Grabias, A., Nowicki, P., & Williamson, D. L. (1996). Mössbauer and X-ray study of the structure and magnetic properties of amorphous and nanocrystalline $Fe_{81}Zr_7B_{12}$ and $Fe_{79}Zr_7B_{12}Cu_2$ alloys. *J. Appl. Phys.*, *79*, 993–1003. DOI: 10.1063/1.360885.
11. Gondro, J., Świerczek, J., Rzącki, J., Ciurzyńska, W., Olszewski, J., Zbroszczyk, J., Błoch, K., Osyra, M., & Łukiewska, A. (2013) Invar behaviour of NANOPERM-type amorphous Fe-(Pt)-Zr-Nb-Cu-B alloys. *J. Magn. Magn. Mater.*, *341*, 100–107. DOI: 10.1016/j.jmmm.2013.04.009.
12. Błachowski, A., & Wdowik, U. D. (2012). Transition metal impurity effect on charge and spin density in iron: *Ab initio* calculations and comparison with Mössbauer data. *J. Phys. Chem. Solids*, *73*, 317–323. DOI: 10.1016/j.jpcs.2011.10.017.10.1016/j.jpcs.2011.10.017.